Spectral behavior of the three-photon absorption coefficient in ionic crystals

I. M. Catalano, A. Cingolani, and M. Lepore
Dipartimento di Fisica dell'Università di Bari, via G. Amendola 173, 70126 Bari, Italy
(Received 21 June 1988)

The three-photon absorption (ThPA) coefficient value at a fixed excitation energy and its frequency dependence in a large energy range have been measured in RbI, CsI, and NaI. Experimental results can be qualitatively and quantitatively described by a parametric formula with mixed spectral dependence, indicating the simultaneous contribution of four different transition mechanisms to the ThPA transition amplitude. A comparison between experimental and various theoretical ThPA line shapes has also been carried out.

Recently, the first expermental evidences of three-photon absorption (ThPA) spectroscopy for both exciton[1,2] and direct interband[3] transitions have been reported in the literature. As regards interband transitions, the ThPA coefficient (α_3) line shapes measured for two different alkali-halide crystals (KI and RbI) in a large excitation energy range have shown that the α_3 spectral behavior can be fully described by the parametric equation:

$$\alpha_3=\sum_{m=0}^{3} C_m(3\hbar\omega_3-E_g)^{m+1/2} \tag{1}$$

containing four different terms, their energy dependences being predicted on the grounds of ThPA selection rules. In particular, the $(3\hbar\omega_3-E_g)^{1/2}$, $(3\hbar\omega_3-E_g)^{3/2}$, $(3\hbar\omega_3-E_g)^{5/2}$, and $(3\hbar\omega_3-E_g)^{7/2}$ dependences have been attributed to ThPA transitions of allowed-allowed-allowed (a-a-a), allowed-allowed-forbidden (a-a-f), allowed-forbidden-forbidden (a-f-f), and forbidden-forbidden-forbidden (f-f-f) type, respectively.[4,5] On the other hand, comparing experimental and theoretical α_3 line shapes has shown that in the above-mentioned large-gap materials, the complete spectral behavior could correctly be described by perturbative models assuming that all four ThPA transition mechanisms [depending on selection rules (and therefore on the right choice of matrix element)] contribute simultaneously to the three-photon transition amplitude (although with different weights at $3\hbar\omega_3$ different values). It is worth noting that only for one of the two investigated materials (KI) has it been possible to give a quantitative α_3 line shape with relative parametric formula C_m coefficient values. In fact, up to now α_3 measurements at fixed frequencies have only been done for a small number of solids not including RbI (see Table V of Ref. 5).

The aim of this work is to test the general validity of the interband ThPA line shape and to obtain the C_m coefficient values for other alkali-halide crystals. For this purpose, the α_3 value has been measured in RbI and CsI at a fixed frequency and its frequency dependence has been investigated in both the above-mentioned materials and also in NaI.

The α_3 coefficient values at $\hbar\omega_3=2.34$ eV have been measured in RbI [$E_g(80\ \text{K})=6.1$ eV] and CsI [$E_g(10\ \text{K})=6.37$ eV] at 80 and 10 K, respectively. High-quality crystals were selected to prevent damage from high-power density excitation and to avoid dependence on sample purity degree. Measurements have been carried out by means of the comparative nonlinear luminescence technique.[6] In fact, keeping the appropriate experimental conditions and knowing the α_2 two-photon absorption (TPA) coefficient, this approach allows one to determine the α_3 ThPA coefficient, by comparing L_n ($n=2,3$) luminescence signals:

$$L_n=K_n\eta_n\alpha_n I_n^n d(1-\beta_n d)(1-\tfrac{1}{2}\alpha_L d) \tag{2}$$

excited by two- and three-photon absorption. In formula (2), I_n is the exciting photon flux at $\hbar\omega_n$, α_n is the n-photon absorption coefficient at $\hbar\omega_n$ frequency, β_n is the one-photon absorption coefficient at the same frequency, d is the sample thickness, α_L is the one-photon absorption at the ω_L luminescence frequency, K_n is the calibrating constant for the experimental configuration used in detecting the luminescence, and η_n is the quantum efficiency relative to n-photon absorption.

In particular, when (i) the photon energies of the excitation fluxes I_2 and I_3 are such that $2\hbar\omega_2=3\hbar\omega_3$, and, consequently, the same quantum efficiency can be assumed in both absorption processes ($\eta=\eta_2=\eta_3$); (ii) the β_3 coefficient is actually negligible; and (iii) the experimental configuration is arranged so that it is possible to assume $k_2=k_3$, the α_3 value can be obtained directly by the ratio L_3/L_2:

$$\alpha_3=\frac{L_3}{L_2}\frac{I_2^2}{I_3^3}\alpha_2(1-\beta_2 d)\ . \tag{3}$$

In both RbI and CsI the two- and three-photon luminescence was excited by the third ($\hbar\omega_2=3.51$ eV) and the second ($\hbar\omega_3=2.34$ eV) harmonic of a Q-switched Nd:YAG (yttrium aluminum garnet) laser with 13-nsec pulse duration and 100-MW maximum peak power. The light of these high-power laser beams was not, however, uniformly distributed over their cross sections, and so much care was taken to reduce and test the influence of

this nonuniformity of the beams on the α_3 values. Two- and three-photon absorption was detected in both RbI and CsI via the self-trapped exciton (STE) luminescence. In fact, in alkali halides the dominant intrinsic decay channels of electronic excitations are luminescence bands of STE.[7] Both the L_2 and L_3 luminescence signals were measured at $\hbar\omega_L = 3.94$ eV for RbI and at $\hbar\omega_L = 3.67$ eV for CsI. The same experimental configuration and the same detection apparatus as those described in Ref. 7, were used to monitor L_2 and L_3 luminescence signals. Moreover by assuming $\beta_2 \cong 0.92$ cm^{-1}, $\beta_3 = 0$, $\alpha_2 = 5.08 \times 10^{-3}$ cm/MW (Ref. 8), and $d = 0.5$ cm for RbI, and $\beta_2 \cong 0.92$ cm^{-1}, $\beta_3 = 0$, $\alpha_2 = 6 \times 10^{-3}$ cm/MW (Ref. 9), and $d = 0.5$ cm for CsI, and by using the experimental results reported in the insets of Figs. 1 and 2 the following α_3 values:

$$\alpha_3^{\mathrm{RbI}} = (8.6 \pm 1.1) \times 10^{-4} \text{ cm}^3/\text{GW}^2 ,$$

$$\alpha_3^{\mathrm{CsI}} = (6.3 \pm 0.8) \times 10^{-4} \text{ cm}^3/\text{GW}^2 ,$$

have been obtained for RbI and CsI at $\hbar\omega_3 = 2.34$ eV. It must be noted that an analogous α_3 measurement cannot be done for NaI, because no α_2 value at a fixed frequency is available in literature.

The α_3 spectral dependencies in RbI, CsI, and NaI [E_g (10 K) = 5.84 eV] were measured near and far from the energy gap (for RbI, 50 meV $\leq 3\hbar\omega_3 - E_g \leq 1815$ meV; for CsI, 50 meV $\leq 3\hbar\omega_3 - E_g \leq 1545$ meV; and for NaI, 50 meV $\leq 3\hbar\omega_3 - E_g \leq 1600$ meV) at 10 K for CsI and NaI and at 80 K for RbI. The α_3 line shape was measured by monitoring the STE luminescence (at the above-reported $\hbar\omega_L$ energies for RbI and CsI and at $\hbar\omega_L = 3.67$ eV for NaI) induced by simultaneous absorption of three identical photons, at different $\hbar\omega_3$ excitation frequencies. The experimental setup was similar to that reported in Ref. 3. The ThPA spectra were obtained by means of a Quantel Datachrome dye laser (pulse duration: 9 nsec; maximum peak power for Rhodamine-6G approximately equal to 30 MW/cm^2) pumped by the second and third harmonics of an Nd:YAG laser. Five efficient dyes were used: Coumarine-480 and -500 for the high-energy side of the spectra and Rhodamine-6G and -B and DCM for low energies. The emitted radiation was detected by a 60-ER response photomultiplier tube, while the incident beam was monitored by a fast response photodiode. Both signals were stored and processed by a computer data acquisition system. To reduce the effects of fluctuations in the input beam intensity, a ratio of the photomultiplier signal to the third power of the monitor signal was used. Moreover, the cubic behavior of the detected luminescence signal versus excitation intensity was checked at each experimental point and, for each of them, different measurement runs were carried out. The experimental accuracy was within about 25% for each run. The ThPA spectra reported here have been obtained by measuring α_3 every 50 meV on average. It is worth noting that the alkali-halide crystals were well suited for our studies because (a) their high STE luminescence efficiency allows the ThPA processes to be studied by utilizing nsec dye laser sources, and (b) their large gaps enable one to use dyes which emit radiation in the visible range and which

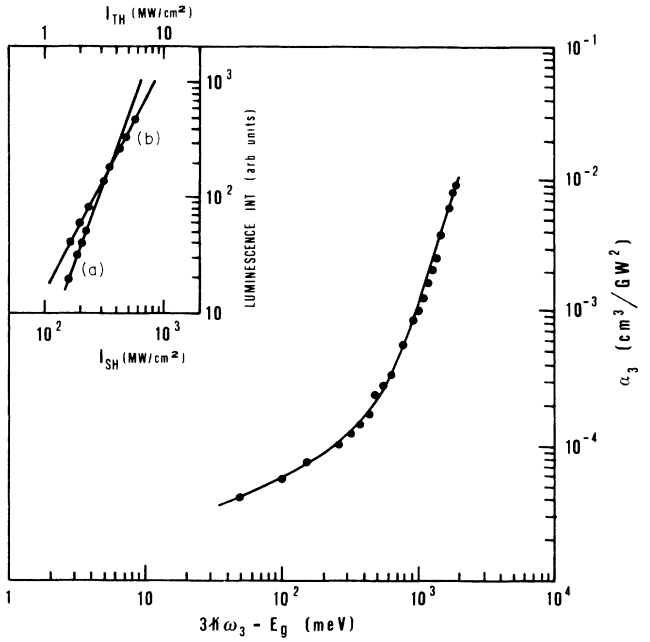

FIG. 1. α_3 (cm^3/GW^2) three-photon absorption coefficient vs $3\hbar\omega_3 - E_g$ for RbI crystal. The solid line is the best fit curve obtained by means of Eq. (1). The dots indicate experimental results. (The χ^2 value for degree of freedom is 0.13 and the fit probability is 0.999.) The inset shows RbI luminescence intensity at $\hbar\omega_L = 3.94$ eV vs laser input peak power: Curve (a) Nd:YAG second-harmonic (SH) excitation; curve (b) Nd:YAG third-harmonic (TH) excitation.

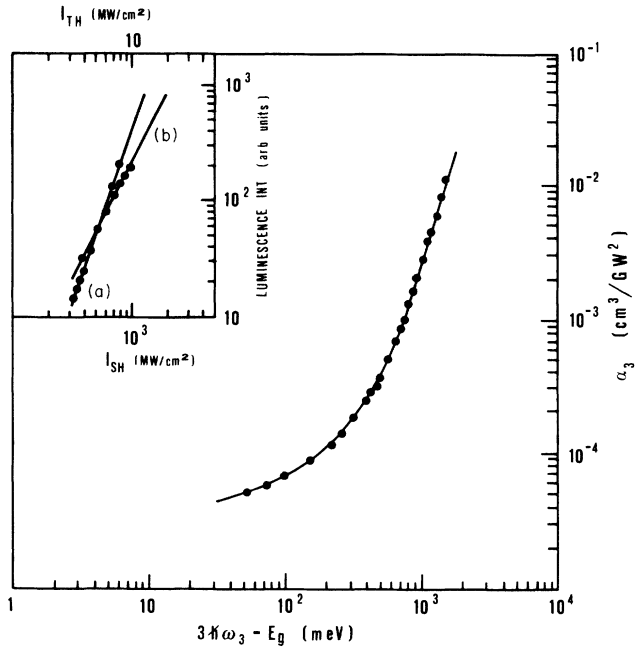

FIG. 2. The same as in Fig. 1 for CsI crystal. (The χ^2 value for degree of freedom is 0.15 and the fit probability is 0.999.) In the inset, the CsI luminescence intensity has been detected at $\hbar\omega_L = 3.67$ eV.

have, as it is well known, the highest available peak power.

The ThPA line shapes (dots) of RbI, CsI, and NaI versus $(3\hbar\omega_3 - E_g)$ have been reported in Figs. 1, 2, and 3, respectively. The RbI and CsI α_3 curves in Figs. 1 and 2 have been obtained by normalizing the experimental data with the α_3 values measured beforehand at $3\hbar\omega_3 - E_g = 0.92$ eV for RbI and at $3\hbar\omega_3 - E_g = 0.65$ eV for CsI. On the contrary, the NaI α_3 curve in Fig. 3 has been expressed in arbitrary units. The RbI, CsI, and NaI experimental line shapes have been fitted with Eq. (1). The results of these fits are shown by the continuous curves in Figs. 1–3. The agreement is good for all materials as shown by the χ^2 values and by the fit probability P reported in the figure captions. Moreover, the C_m coefficient values for RbI and CsI normalized curves have been reported in Table I. The results of these fittings show that all the terms of Eq. (1) play a part in the ThPA spectral dependence. This suggest that all four ThPA mechanisms (*a-a-a*, *a-a-f*, *a-f-f*, and *f-f-f*) depending on the selection rules contribute simultaneously to the ThPA interband transition amplitude in the considered energy range but with different weights at different $3\hbar\omega_3$ values. Moreover, the C_m coefficients for RbI and CsI are very similar to the ones already found in KI[3] thus confirming the validity of the functional form (1) in describing α_3 frequency dependence.

Our previous works on two-photon interband transitions in different crystals[10] and three-photon ones in KI[3] have shown that no theoretical model proposed to calculate TPA and ThPA coefficients can correctly describe the α_3 and α_2 line shapes in a large energy range. Conversely, for both TPA and ThPA processes, the results of theoretical models considering transitions of just the allowed type seem to agree reasonably well with experimental data in the energy region near the direct optical gap. Confirming this, Figs. 4(a) and 4(b) give a comparison between theoretical and experimental line shapes for RbI and CsI, respectively. The theoretical curves (*a*, *b*, and *c*) are related to the three different theoretical approaches used to calculate α_3. In particular, curve *a* comes from a four-band model which uses *a-a-a* transitions (formula 16 of Ref. 11), curve *b* is obtained from a two-band model with *a-f-f* transitions (formula 20 of

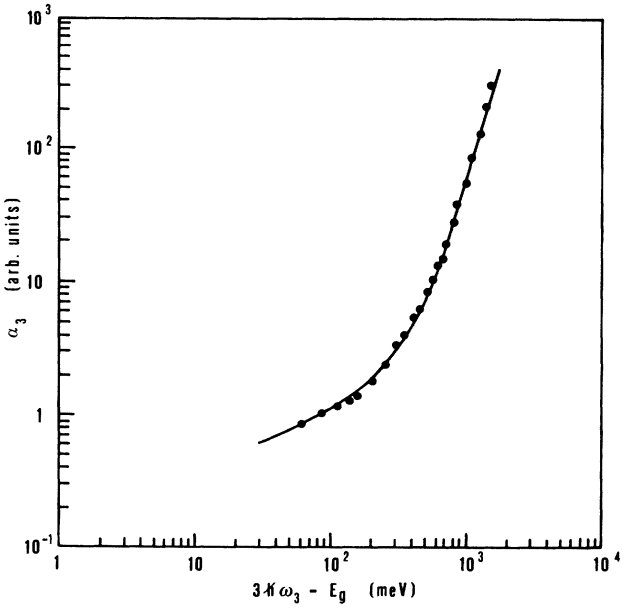

FIG. 3. α_3 (arbitrary units) three-photon absorption coefficient vs $3\hbar\omega_3 - E_g$ for NaI crystal. The solid line is the best fit curve obtained by means of Eq. (1). The dots indicate experimental results. (The χ^2 value for degree of freedom is 0.34 and the fit probability is 0.996.)

TABLE I. Values of the parametric formula (1) C_m coefficients for RbI and CsI.

Material	C_1	C_2	C_3	C_4
RbI	0.58×10^{-5}	0.09×10^{-8}	0.16×10^{-11}	0.27×10^{-13}
CsI	0.66×10^{-5}	0.14×10^{-8}	0.11×10^{-11}	0.62×10^{-13}

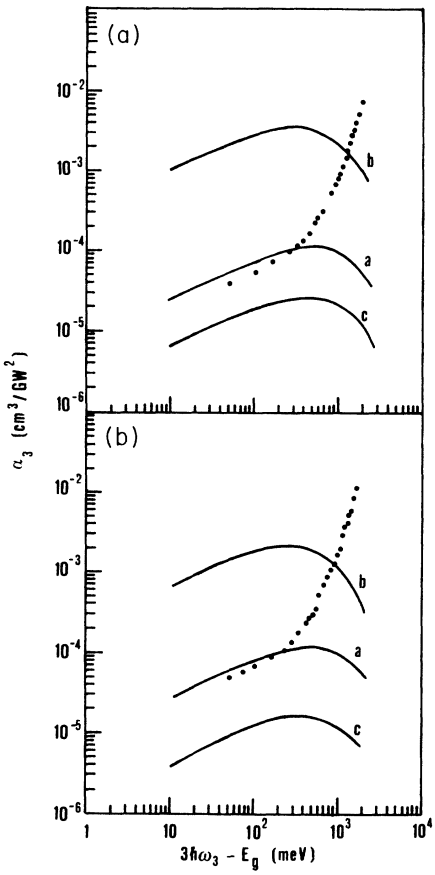

FIG. 4. (a) Quantitative comparison between the α_3 experimental (dots) and theoretical (solid lines) line shapes for RbI. Solid lines *a* and *b* have been calculated by means of four- and two-band models, respectively; while the *c* one has been calculated by means of a nonperturbative model. In the theoretical calculations the following physical parameters have been used: $E_g = 6.1$ eV at 80 K, $E_m = 6.95$ eV, $E_n = 8.24$ eV, $n = 1.731$, $m_c = 0.88 m_0$, $m_v = 0.5 m_0$, and $|P_{cv}|^2 = \frac{3}{4} E_g (m_0^2/m_{cv}^*)$. (b) The same for CsI crystal. The physical parameter used in the theoretical calculations has been $E_g = 6.37$ eV at 10 K, $E_m = 6.5$ eV, $E_n = 8.69$ eV, $n = 1.62$, $m_c = 0.77 m_0$, $m_v = m_0$, and $|P_{cv}|^2 = \frac{3}{4} E_g (m_0^2/m_{cv}^*)$.

Ref. 4), and curve c is calculated by means of a nonperturbative approach (formula 41 of Ref. 12). In the first model, the calculation has been carried out by using the third-order time-dependent perturbation theory and assuming two higher conduction bands for the intermediate states, in the second model the α_3 calculation has been developed using the S matrix and the second quantization formalism; while, in the third case, the transition rate has been calculated between Stark-shifted levels, taking all orders of the perturbation expansion into account.[8] All these models characterized by a dominant $(3\hbar\omega_3 - E_g)^{1/2}$ spectral dependence neglect the excitonic contribution in the continuum.

It is evident that for RbI and CsI a satisfactory qualitative agreement between the α_3 experimental line shape and the ones obtained by the three theoretical models considered here has only been found for $3\hbar\omega_3 - E_g$ ranging between approximately 50 and 200 meV above the band gap. In this range, the four-band model also shows good quantitative agreement with the experimental data that, on the contrary, are greatly overestimated by the two-band model and underestimated by the nonperturbative one. On the other hand, in the range beyond 200 meV above the energy gap, the experimental and theoretical line shapes for RbI and CsI do not agree at all. It must be noted that the α_3 values measured in the initital region up to approximately 50 meV result to be greater than the theoretical ones calculated by the four-band model. This mismatching can be ascribed to the excitonic contribution in the continuum.[3]

In conclusion, the general validity of parametric formula (1) to quantitatively and qualitatively describe the three-photon spectrum in ionic crystals have been proved, indicating the simultaneous contribution of four possible transition mechanisms, depending on selection rules, to the ThPA transition amplitude. Moreover a satisfactory quantitative agreement between experimental data and four-band model theoretical predictions has been demonstrated for ThPA transitions in an energy range near the fundamental optical gap.

The authors are very grateful to Mr. M. Sibilano for his technical assistance. This work was partially supported by the Ministero della Pubblica Istruzione (Italy).

[1]F. Beerwerth and D. Frohlich, Phys. Rev. Lett. **55**, 2603 (1985).
[2]F. Beerwerth and D. Frohlich, Phys. Rev. Lett. **57**, 1344 (1986).
[3]I. M. Catalano, A. Cingolani, R. Cingolani, and M. Lepore, Phys. Rev. B **38**, 3438 (1988).
[4]A. I. Bobrysheva and S. A. Moskalenko, Fiz. Tekh. Poluprovdn. **3**, 1601 (1969) [Sov. Phys.—Semicond. **3**, 1347 (1970)].
[5]V. Nathan, A. H. Guenther, and S. S. Mitra, J. Opt. Soc. Am. B **2**, 294 (1985).
[6]I. M. Catalano and A. Cingolani, J. Appl. Phys. **50**, 5638 (1979); I. M. Catalano, A. Cingolani, M. Ferrara, and M. Lugara, Opt. Acta **27**, 625 (1980).
[7]W. B. Fowler, in *Physics of Color Centers*, edited by W. B. Fowler (Academic, New York, 1968).
[8]P. Liu, W. L. Smith, H. Lotel, J. H. Bechtel, N. Bloembergen, and R. S. Adhav, Phys. Rev. B **17**, 4260 (1978).
[9]C. H. Chenm, M. P. McCann, and J. C. Wang, Solid State Commun. **61**, 559 (1987).
[10]I. M. Catalano, A. Cingolani, and M. Lepore, Phys. Rev. B **33**, 7270 (1986); I. M. Catalano, R. Cingolani, and M. Lepore, Solid State Commun. **60**, 385 (1986). I. M. Catalano, A. Cingolani, R. Cingolani, and M. Lepore, Phys. Scr. **37**, 578 (1988).
[11]F. Bassani and A. R. Hassan, Nuovo Cimento **7B**, 313 (1972).
[12]L. V. Keldysh, Zh. Eksp. Teor. Fiz. **47**, 1945 (1964) [Sov. Phys.—JETP **20**, 1307 (1965)].